

Studies on room temperature multiferroic properties of $x\text{Bi}_{0.5}\text{Na}_{0.5}\text{TiO}_3-(1-x)\text{NiFe}_2\text{O}_4$ ceramics

Liguang Wang¹ · Changming Zhu¹ · Hui Luo² · Songliu Yuan¹

Received: 12 November 2014 / Accepted: 14 May 2015 / Published online: 24 May 2015
© Springer Science+Business Media New York 2015

Abstract Multiferroic ceramics $x\text{Bi}_{0.5}\text{Na}_{0.5}\text{TiO}_3-(1-x)\text{NiFe}_2\text{O}_4$ ($x=0-1$) have been prepared by a sol–gel method. Crystal structures were investigated by X-ray diffraction. The results show the samples are pure phases and increasing $\text{Bi}_{0.5}\text{Na}_{0.5}\text{TiO}_3$ content induces a gradual phase transformation from spinel to perovskite structure. Scanning electron microscopy micrographs also present the size and structure of the samples. Results from energy dispersive spectrometer confirm the stoichiometry of the compound. Both of the data are proved to agree with the results of X-ray diffraction. All of the samples display the evident ferromagnetic properties at 300 K and the saturation magnetization almost linearly varies with the increasing of x . The room temperature polarization–electric field loops were examined. Compared with pure NiFe_2O_4 , superior ferroelectric properties are obtained with increasing maximum of polarization as the content of $\text{Bi}_{0.5}\text{Na}_{0.5}\text{TiO}_3$ increases. Dielectric properties were also studied. The dielectric constant is proved to increase as $\text{Bi}_{0.5}\text{Na}_{0.5}\text{TiO}_3$ content increases at room temperature and the dielectric loss decreases as $\text{Bi}_{0.5}\text{Na}_{0.5}\text{TiO}_3$ doped in NiFe_2O_4 . In addition, some of samples exhibit the effect of magnetoelectric coupling.

Keywords Ceramic composites · Magnetic materials · Ferroelectrics · Dielectrics · Sol–gel preparation

✉ Songliu Yuan
yuansl@hust.edu.cn

¹ School of Physics, Huazhong University of Science and Technology, Wuhan 430074, People's Republic of China

² School of Optical and Electronic Information, Huazhong University of Science and Technology, Wuhan 430074, People's Republic of China

1 Introduction

Multiferroicity is generally defined as the coupling between different ferroic orders with one subset producing the magnetoelectric or the other magnetodielectric effect. Thus, relying on this, multiferroic materials which exhibit more than one spontaneous electric, magnetic and elastic order simultaneously have been one of the hot research topics because of their potential applications in memory devices, sensors, optical filters and so on [1–3]. The coexisting ferroic orders can couple in the same phase but to our knowledge, the composite multiferroics may have a larger magnetoelectric effect which is important for application, than their single phase counterpart, generally. Therefore, it will be more interesting to study the composites based on ferroelectric–ferromagnetic, ferroelectric–ferrimagnetic or others.

It has been proved that the perovskite structure is stable and the coexistence of ferromagnetism and ferroelectricity can be established [4, 5]. $\text{Bi}_{0.5}\text{Na}_{0.5}\text{TiO}_3$ (BNT) is a lead-free rhombohedral perovskite-type ferroelectric materials with Curie temperature $T_c=320$ °C. It can form solid solutions with other perovskite-type materials such as BiFeO_3 , BaTiO_3 [6, 7]. Nevertheless, systematic study on BNT formed solid solution with the spinel-type materials is still lacking.

Except for perovskites, spinel-type materials have also received much attention because of its importance for technological application such as ferrimagnetic insulators just like most spinel ferrites. Moreover, spinel is a complex crystal structure with many degrees of freedom available to some physical properties. Among the spinel ceramics, magnetic NiFe_2O_4 (NFO) is a well-studied ferrite compound with magnetic ordering temperature well above room temperature [8, 9]. It is soft magnetic with an inverse spinel structure and the ferrimagnetism originates from magnetic moments of antiparallel spins between Fe^{3+} ions at tetrahedral sites and Ni^{2+} ions

at octahedral sites [10, 11]. Therefore, in solid solutions, NFO can act as a magnetic source and the potential additive absolutely to combine perovskites for the strong magnetic-electric properties.

Based on the above description, it will be meaningful to prepare $x\text{Bi}_{0.5}\text{Na}_{0.5}\text{TiO}_3-(1-x)\text{NiFe}_2\text{O}_4$ (BNT0-NFO) multiferroic composite ceramic systems. In this work, we focus on the structure, magnetic, ferroelectric and dielectric properties which have been systematically studied in the BNT0-NFO solid solutions with $x=0, 0.1, 0.2, 0.3, 0.4, 0.5, 0.6, 0.7, 0.8, 0.9$ and 1. The enhanced multiferroics properties can be clearly observed in the intensively report below.

2 Experiment

BNT0-NFO ($x=0-1$) ceramics were synthesized by a sol-gel method [12] using nitrates as metal precursors. First, citric acid [$\text{C}_6\text{H}_8\text{O}_9$] was dissolved in distilled water as a complexant. Bismuth nitrate [$\text{Bi}(\text{NO}_3)_3 \cdot 5\text{H}_2\text{O}$], sodium nitrate [NaNO_3], nickel nitrate [$\text{Ni}(\text{NO}_3)_2 \cdot 6\text{H}_2\text{O}$], iron nitrate [$\text{Fe}(\text{NO}_3)_3 \cdot 9\text{H}_2\text{O}$] and tetrabutyl titanate [$\text{C}_{16}\text{H}_{36}\text{O}_4\text{Ti}$] were dissolved into the solution of citric acid in stoichiometric proportions to form the sol. The solution was adjusted to a pH value of 4–7 by adding ammonia. Then, the solution was evaporated to form a gel. After that the gel was dried and burned until the combustion process was completed. Subsequently, the mixture was calcined at 550 °C for 5 h to form the precursor powder, which was reground and pressed into the pellets. The pellets were 1 mm in thickness and 10 mm in diameter. Finally, the pellets were sintered at 1000 °C for 3 h. Electrodes with 6 mm in diameter were applied to both surfaces to measure electrical properties with silver paste.

Crystal structures of the samples were investigated by X-ray diffraction (XRD) and the XRD data were collected on a Panalytical X'pert PRO X-ray diffractometer. Micrographs and the stoichiometry are displayed by scanning electron microscopy (SEM) and energy dispersive spectrometer (EDS) with a JSM-5610LV. Magnetic properties were studied using the Physics Property Measurement System (PPMS). Ferroelectric properties were measured using a commercial ferroelectric test system (PremierII, Radiant Technologies) and the dielectric properties were measured by PST-2000H.

3 Result and discussion

The XRD patterns of BNT0-NFO ($x=0-1$) are presented in Fig. 1, which confirms the presence of both perovskite and spinel phases corresponding to BNT0 and NFO, respectively. The patterns show that there is no traces of other phases. More

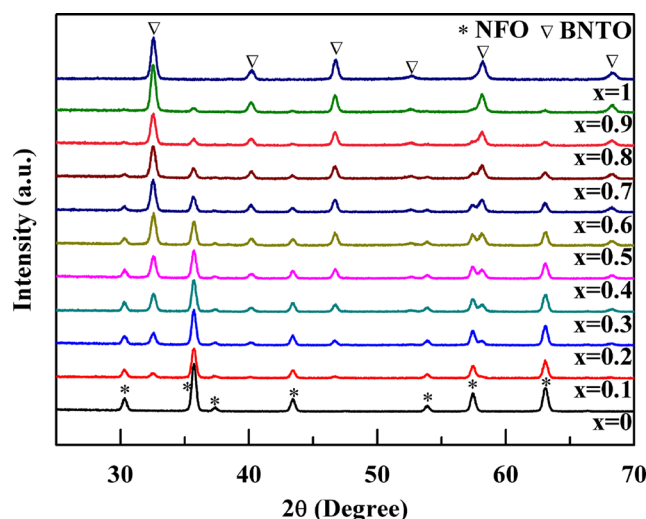


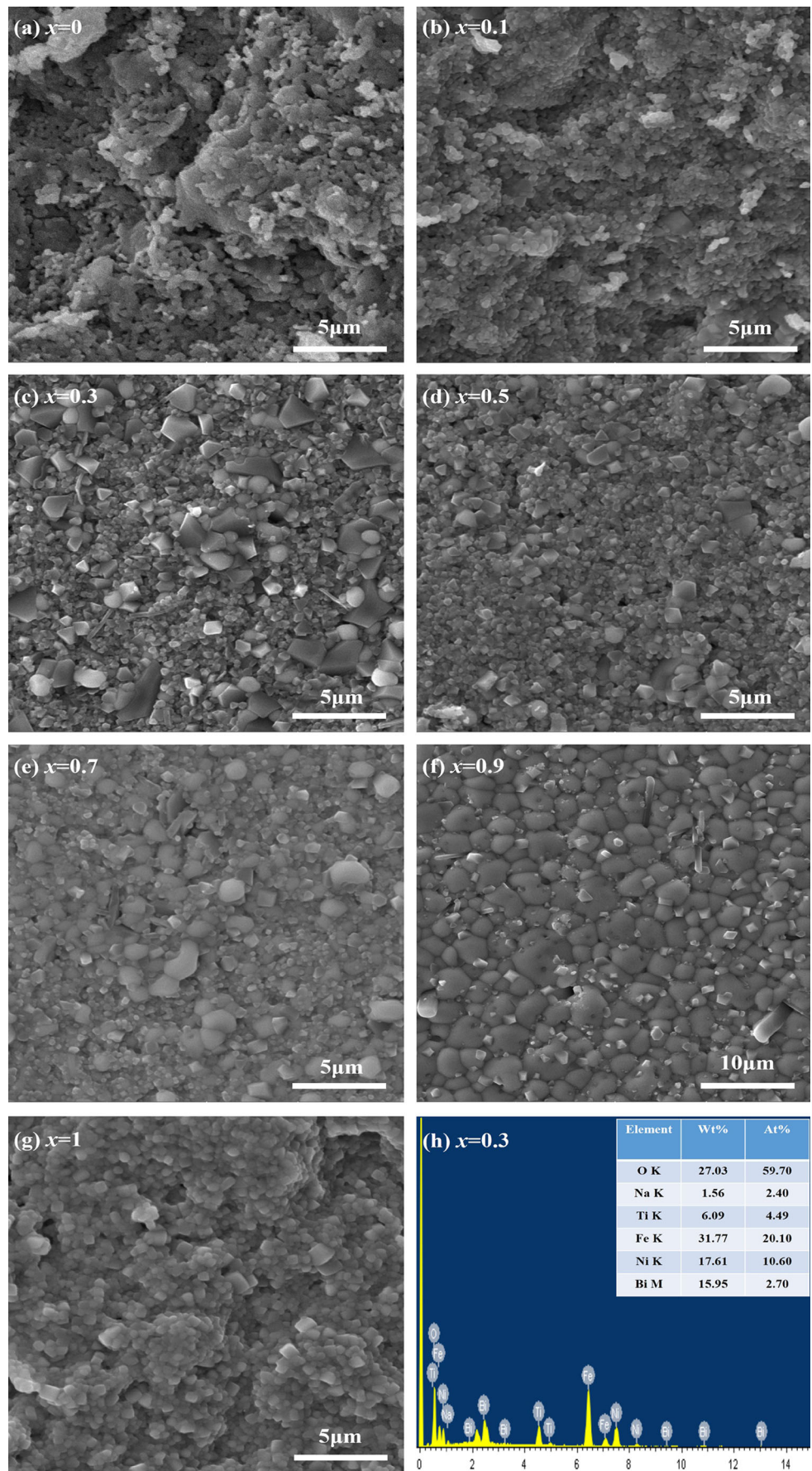
Fig. 1 X-ray diffraction patterns of $x\text{Bi}_{0.5}\text{Na}_{0.5}\text{TiO}_3-(1-x)\text{NiFe}_2\text{O}_4$ ($x=0-1$)

important, even with $x=0.1$ the diffraction peaks of BNT0 are still observable and the intensity of BNT0 peaks increases while that of NFO peaks decreases with BNT0 content increasing. The surface morphology of samples are present in Fig. 2(a–g). With increasing the doping content of BNT0, the morphology of samples change from loose spinel only, then coexistence with bigger grain of perovskite and smaller spinel grain, to dense BNT0 which is similar to other reports [13, 14]. EDS result confirms the stoichiometry of the 0.3BNT0-0.7NFO ceramic and prove the sample pure, as shown in Fig. 2(h).

Figure 3(a) displays the typical magnetic hysteresis loops of BNT0-NFO for different content at 300 K. All of the samples show saturated loops which reveal the room temperature ferromagnetism of the composites. The presence of magnetic properties should be attributed to the ordered magnetic structure of NFO in the samples. Notably, as the content of BNT0 increases, the saturation magnetization (M_s) declines. Figure 3(b) plots the variation of M_s with the doping content of BNT0 and the linear fit for the different composites. The decrease of the M_s is almost linear as doping content of BNT0 increases. The decrease tendency of M_s is mainly attributed to the dilution effect caused by the phase without magnetism, the magnetic behavior of NFO which is related to Neel theory [15] of ferrimagnetisms and the cation distribution. In two phases system, the individual ferrite grains give contribution to the magnetism and the grains of BNT0 next to the NFO grains break the connection of magnetic grains. That is to say that acting as pores, BNT0 grains break the magnetic circuits, which is in good agreement with the earlier studies [16, 17].

Polarization against electric field (P-E) was measured with 100 Hz at room temperature, as plotted in Fig. 4. From the ferroelectric hysteresis loops of BNT0-NFO for $x=0.6, 0.7$,

Fig. 2 (a–g) SEM micrographs of $x\text{Bi}_{0.5}\text{Na}_{0.5}\text{TiO}_3-(1-x)\text{NiFe}_2\text{O}_4$ ($x=0, 0.1, 0.3, 0.5, 0.7, 0.9$ and 1); (h) micro EDS of $0.3\text{Bi}_{0.5}\text{Na}_{0.5}\text{TiO}_3-0.7\text{NiFe}_2\text{O}_4$



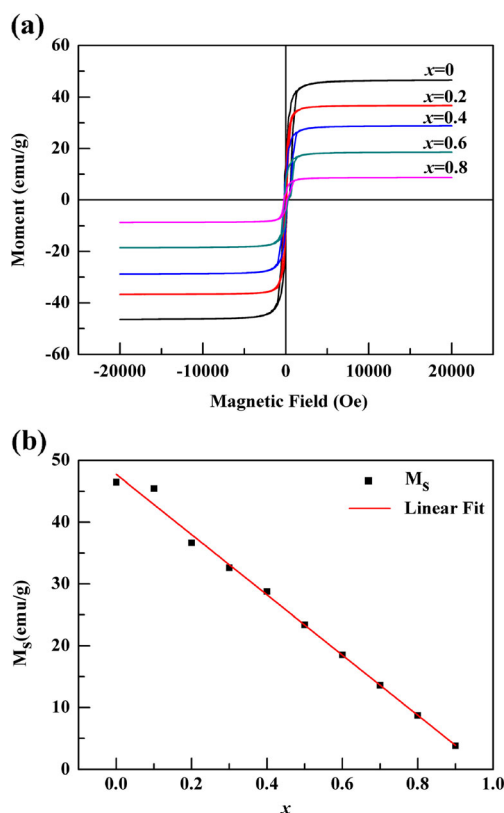


Fig. 3 (a) Magnetic hysteresis loops of $x\text{Bi}_{0.5}\text{Na}_{0.5}\text{TiO}_3-(1-x)\text{NiFe}_2\text{O}_4$ ($x=0, 0.2, 0.4, 0.6$ and 0.8); (b) variation of saturation magnetization of $x\text{Bi}_{0.5}\text{Na}_{0.5}\text{TiO}_3-(1-x)\text{NiFe}_2\text{O}_4$ with x

0.8, 0.9 and 1, ferroelectric behavior is observed without saturation. The ferroelectric hysteresis loops with $x=0-0.5$ are not shown here due to the small enough breakdown voltage. With increasing content of BNT0, the measured maximum of polarization (P_{max}) increase. The P_{max} variation of BNT0-NFO for $x=0.5-1$ is also presented in Fig. 4(f). The higher polarization of the samples is attributed to the lower content of NFO, just because the NFO phase is paraelectric [18]. When BNT0 content reaches to 0.8, the polarization of BNT0-NFO has a slow increase and after that, P_{max} increases sharply with the increasing of BNT0. It suggests that there should be a critical point of x around 0.8. The polarization ability of BNT0-NFO is enhanced once the BNT0 mole ratio is beyond the critical point. In addition, we have also discussed the remanent polarization (P_r). When the content of BNT0 is smaller than 0.9, P_r is low with about $0.5 \mu\text{C}/\text{cm}^2$. With x increasing above 0.8, P_r has an evident increase accompanied with the almost $2 \mu\text{C}/\text{cm}^2$ of $x=1$, which is consistent with P_{max} . From the P-E loops, we can find that samples of BNT0-NFO exhibit weak ferroelectric property at room temperature. The reason may be the voltage drop across the ferrite phase which reduces the net impedance at the interface of BNT0 and NFO. NFO in the composites increases the conductivity, so the ferroelectric property is weak with higher content of NFO and is enhanced when content of BNT0 is increased.

The magnetolectric (ME) coupling effect at room temperature in BNT0-NFO have been demonstrated by electric signal measurement. The P-E loops of different samples measured without and with an external applied magnetic field is shown in Fig. 5. When 5000 Oe is applied, the P-E loops present different deviation from the loops without magnetic field. The values of P_{max} have an increase in the samples especially when x is 0.6. It can be seen as the evidence of ME coupling. The theoretical description of multiferroic properties is complicated because of the coupling interaction between the electric and magnetic properties. Multiferroic materials incorporate both ferroelectric and magnetic phase. However, neither the ferroelectric nor the magnetic phase shows the ME effect, but just the composites of the two phases have the effect. The following may explain it. The ME effect is a result of the piezoelectric effect in the ferroelectric phase and the magnetostrictive effect in the magnetic phase. With a magnetic field applied to BNT0-NFO, the material will be strained and the shape of magnetic phase will be changed. Due to the coupling between the magnetic and ferroelectric domain, the strain would induce a stress, which gives rise to an electric polarization.

Temperature dependence of dielectric constant (ϵ_r) for BNT0-NFO ($x=0.6-0.9$) with various frequency are shown in Fig. 6(a-d). For the samples, dielectric constants increase at low temperature followed by the appearance of peaks at about $320 \text{ }^\circ\text{C}$, which is referred to the ferroelectric transition of BNT0 [19]. With temperature increasing, the increase in dielectric constant is also seen with a sharp increase tendency. It is worth noting that another peak emerges at higher temperature range especially for samples with $x=0.8$ and 0.9 . According to the range of temperature, the peak is at the Curie temperature, which is indicated the phase transition of NFO [20]. What is more, the transition temperature shifts toward to lower temperature as the content of NFO increases. The observed behavior may be attributed to the change of magnetic ordering in NFO. As an effect of vanishing magnetic order on electric order, Landau-Devonshire theory of phase transitions has predicted this type of dielectric anomaly in the magnetolectrically ordered systems [21]. It is consistent with the manipulation of ME interaction, which can induce the shift in magnetic transition temperature due to an electric field. This phenomenon further proves the ME coupling in the samples. In addition, the peak position at $320 \text{ }^\circ\text{C}$ of the samples is not changed with the doping content, which reveals the formation of BNT0 with NFO does not change the phase transition of BNT0 itself.

In addition, temperature dependence of dielectric loss ($\tan \delta$) with various frequency are plotted in Fig. 7(a-d). Especially for samples with $x=0.7-0.9$, the variation of dielectric loss with temperature shows a dielectric anomaly at the temperature range from $350-600 \text{ }^\circ\text{C}$ with evident frequency dispersion of the peaks, which suggests a relaxor-like behavior. It is similar to relaxor ferroelectric materials [22, 23]. According to

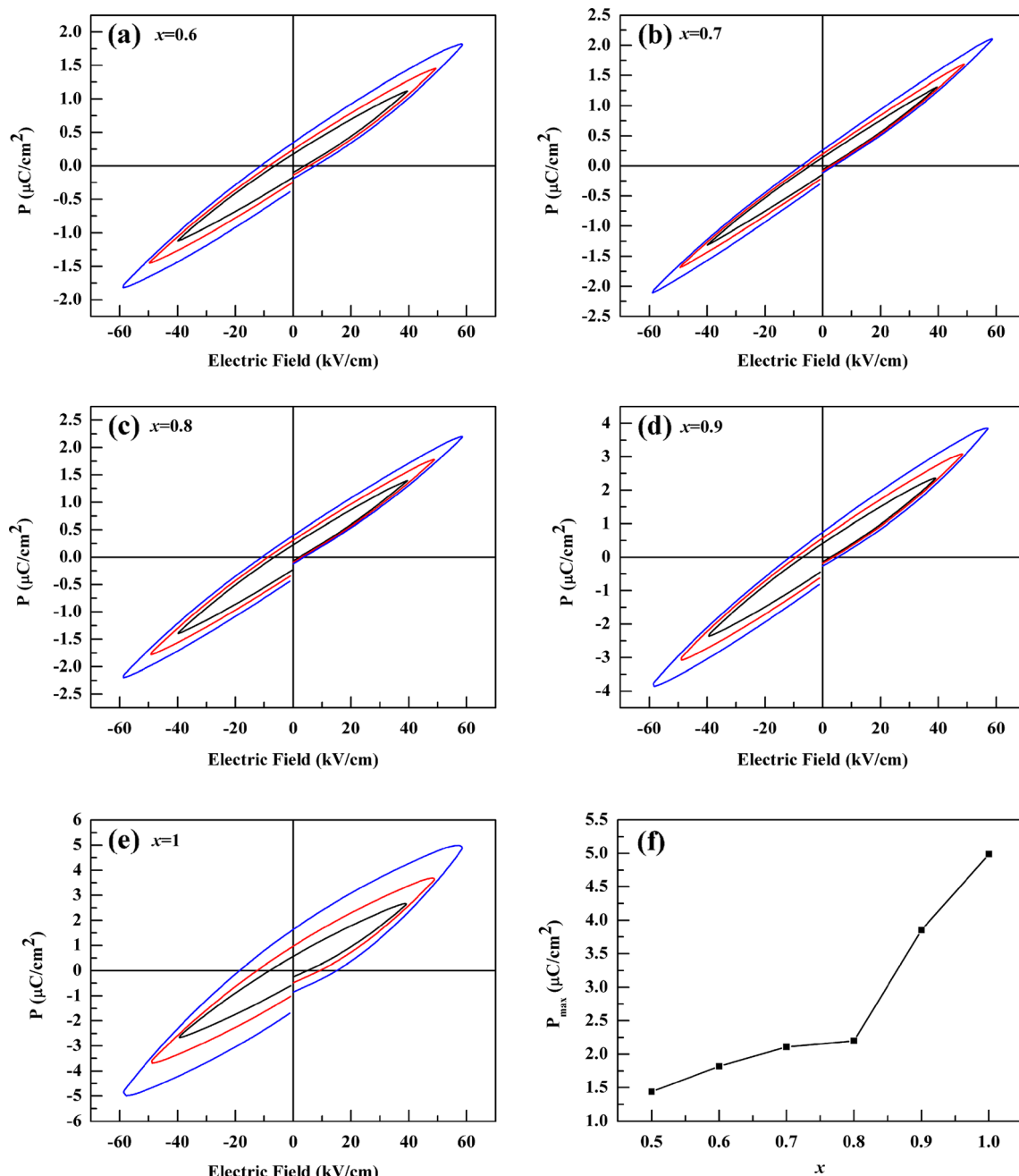


Fig. 4 (a–e) Ferroelectric hysteresis loops of $x\text{Bi}_{0.5}\text{Na}_{0.5}\text{TiO}_3-(1-x)\text{NiFe}_2\text{O}_4$ ($x=0.6, 0.7, 0.8, 0.9$ and 1); (f) the P_{max} variation of $x\text{Bi}_{0.5}\text{Na}_{0.5}\text{TiO}_3-(1-x)\text{NiFe}_2\text{O}_4$ ($x=0.5, 0.6, 0.7, 0.8, 0.9$ and 1) with x

the results of XRD, SEM and EDS, the structure is likely to remain in the original unit cell. The phase transition of BNT0 is still unchanged from the result of dielectric constant. As a normal ferroelectric, pure BNT0 does not present the relaxor features at about 320 °C and this can be proved from Fig. 8. Generally, several reasons have been proposed for this phenomenon, for example, thermal agitation of local polarization fluctuations induced by chemical heterogeneities [24] and formation of fractal clusters inside the normal ferroelectric domains [25]. Commonly, no structural transition is observed

with such dielectric anomaly. Besides, for the magnetoelectrically ordered system, the dielectric anomaly may also appear near the magnetic transition temperature on the basis of Landau-Devonshire theory. Therefore, the possible reasons can be as follows. An interchange of cationic sites of different sizes producing subtle local lattice distortions in the ideal crystal structure exhibits the dielectric anomaly. Another possibility is the coupling result of electric and magnetic order. Of course, further investigation are still needed to reveal the real physical natures of the dielectric anomaly in BNT0-

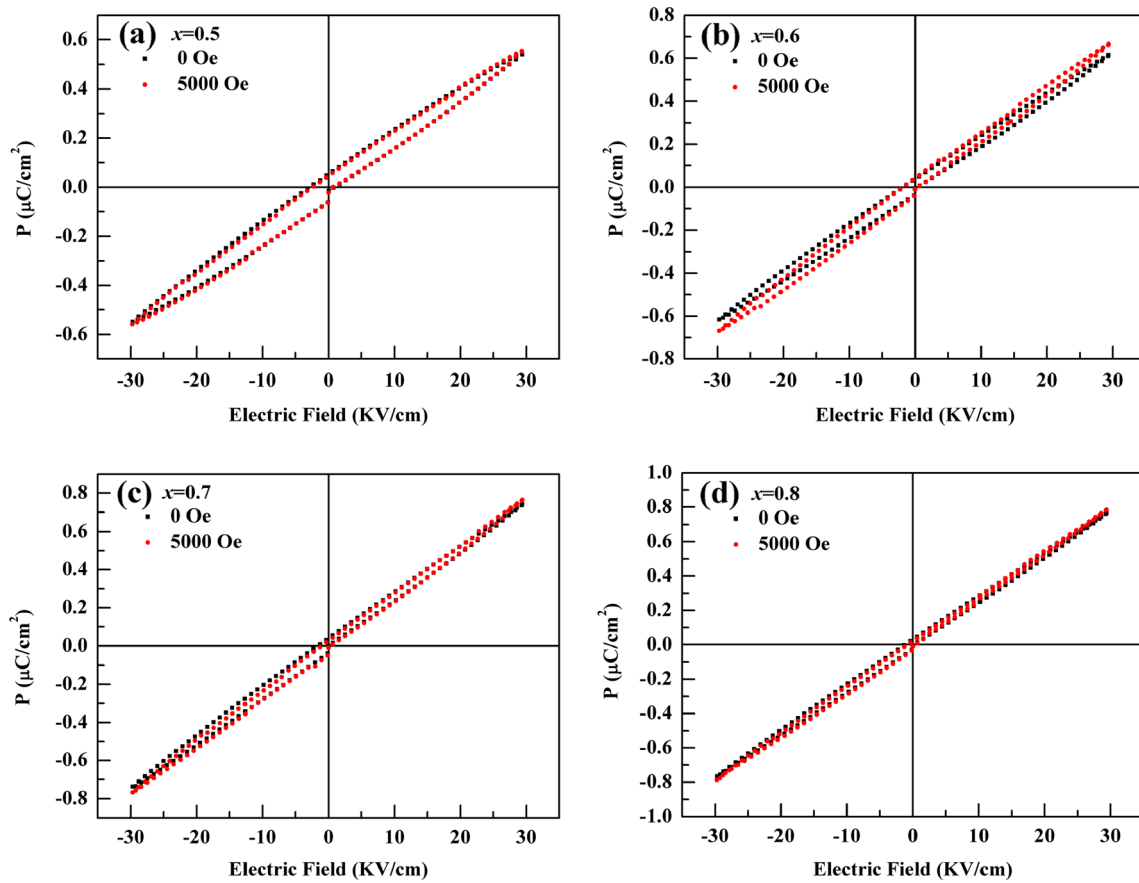
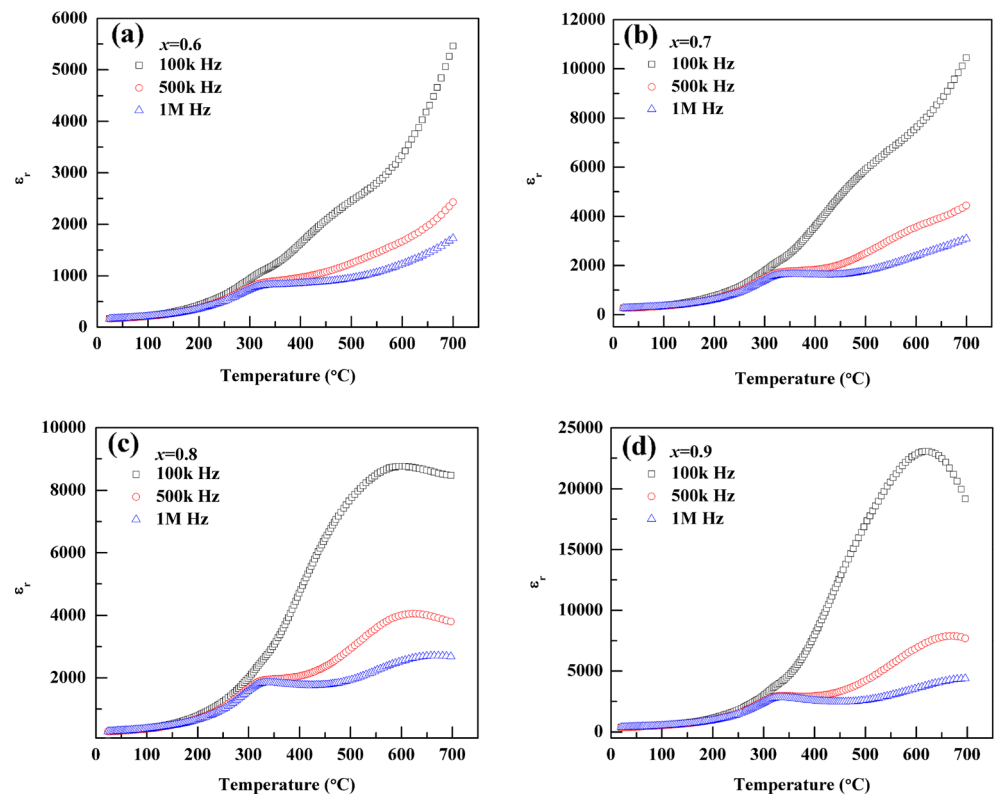


Fig. 5 Polarization against electric field loops for $x\text{Bi}_{0.5}\text{Na}_{0.5}\text{TiO}_3-(1-x)\text{NiFe}_2\text{O}_4$ ($x=0.5, 0.6, 0.7$ and 0.8) without and with a 5000 Oe external magnetic field

Fig. 6 Variation of dielectric constant of $x\text{Bi}_{0.5}\text{Na}_{0.5}\text{TiO}_3-(1-x)\text{NiFe}_2\text{O}_4$ ($x=0.6, 0.7, 0.8$ and 0.9) with temperature



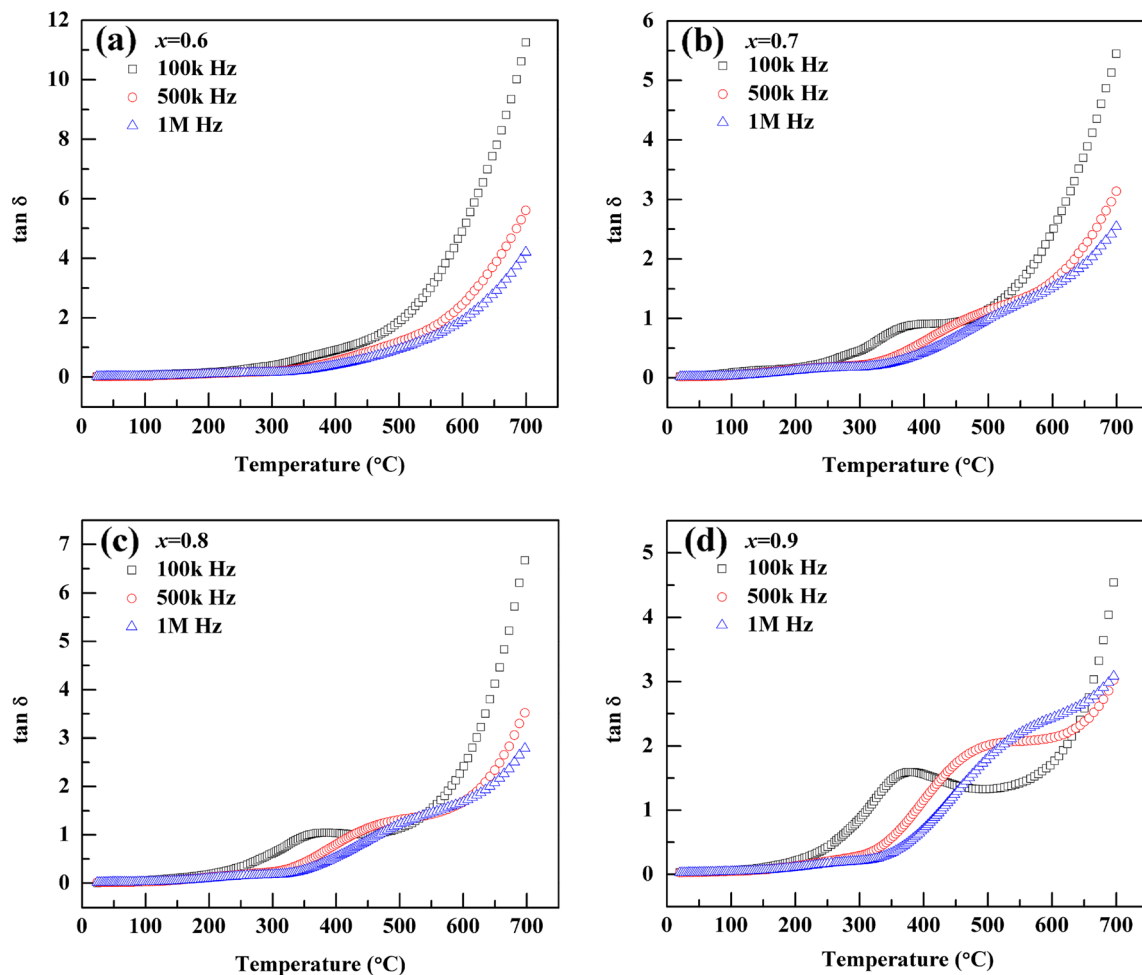


Fig. 7 Variation of dielectric loss of $x\text{Bi}_{0.5}\text{Na}_{0.5}\text{TiO}_3-(1-x)\text{NiFe}_2\text{O}_4$ ($x=0.6, 0.7, 0.8$ and 0.9) with temperature

NFO. What is also needed to pointed out is that the dielectric loss of samples is small enough at room temperature, which also helps the BNTO-NFO composite to be a very useful role for multifunctional application much further.

In order to obtain a deeper insight into the dielectric properties of BNTO-NFO, the variation of dielectric constant with

frequency is shown in Fig. 9(a). The dielectric constant of the different composites ($x=0.6-1$) at room temperature varies with the different content of BNTO and NFO. Dielectric constant with high value at low frequencies decreases sharply with increasing frequency and gradually reaches a constant value at high frequency. This behavior may be caused by

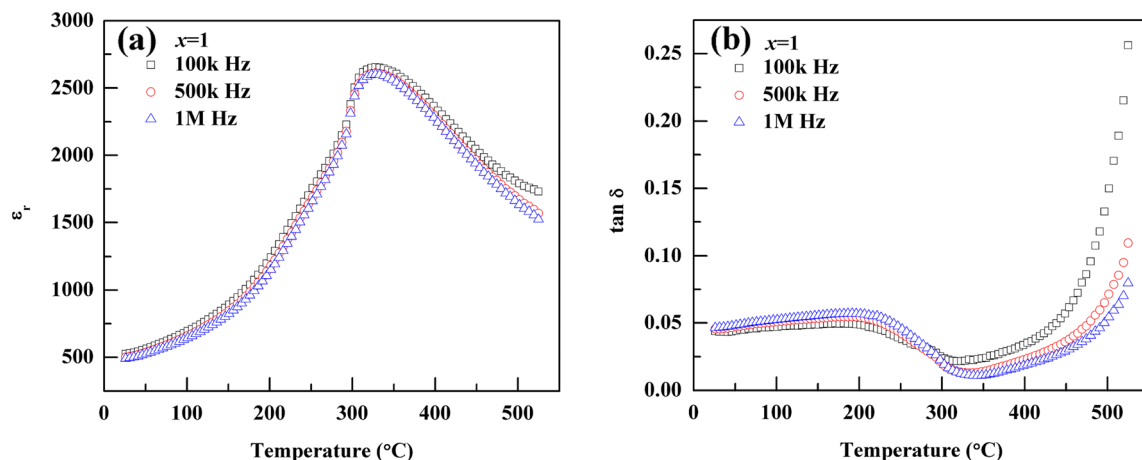


Fig. 8 Variation of dielectric constant (a) and dielectric loss (b) of $\text{Bi}_{0.5}\text{Na}_{0.5}\text{TiO}_3$ with temperature

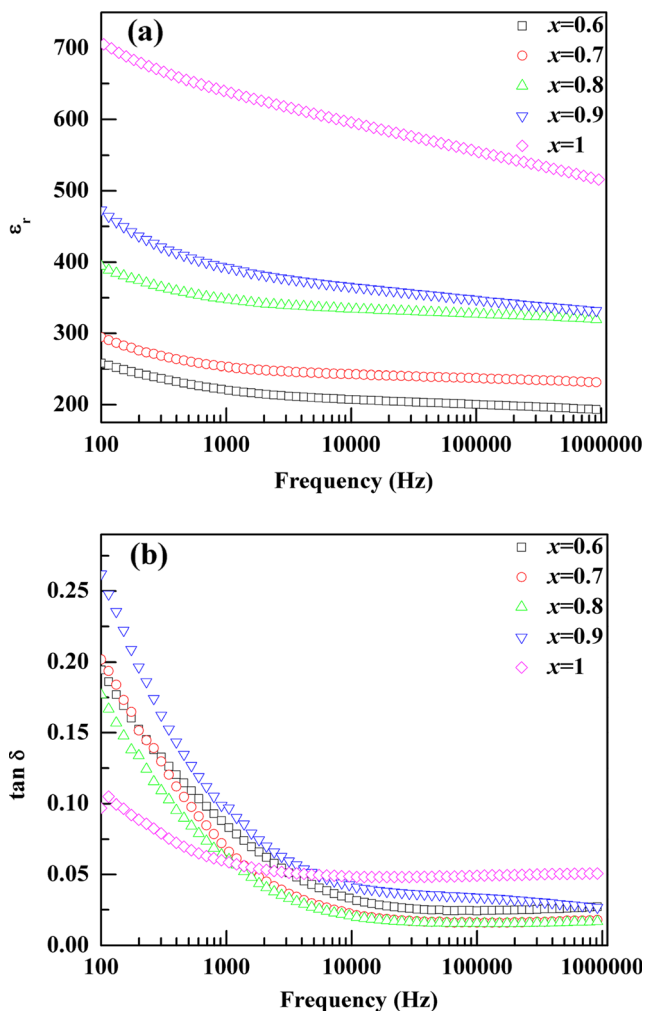


Fig. 9 Variation of dielectric constant (a) and dielectric loss (b) of $x\text{Bi}_{0.5}\text{Na}_{0.5}\text{TiO}_3-(1-x)\text{NiFe}_2\text{O}_4$ ($x=0.6, 0.7, 0.8, 0.9$ and 1) with frequency at room temperature

Maxwell-Wagner effect, which commonly refers to interfacial polarization, occurring in electrically inhomogeneous system [26]. The inhomogeneities in samples of BNT0 and NFO can arise from porosity and grain structure. When an electric current passes through interfaces between two different dielectric media such as the ferrite phase and the ferroelectric phase in our samples, because of the different permittivities, the space charge carriers need finite time to make the axes parallel to the applied electric field. Thus, the behavior of dielectric constant can be understood. We also plot of the variation of dielectric loss with frequency at room temperature in Fig. 9(b). A gradual decrease appears as frequency increases. The dielectric loss represents the dissipation of energy in dielectric system and it is proportional to the imaginary part of dielectric constant. At high range of frequency, space charge polarizability has no influence on dielectric response. Thus, just contributions from ionic, orientation and electronic polarization still remain.

4 Conclusion

In conclusion, multiferroic ceramics of BNT0-NFO are synthesized using the sol-gel method. The structure, magnetic, ferroelectric and dielectric properties of the different samples have been studied. The coexistence of perovskite BNT0 and spinel NFO phases is proved by XRD and SEM, which are pure phases without any impurity. Observations of magnetic and ferroelectric hysteresis loops reveal that the excellent ferromagnetic and ferroelectric properties exist simultaneously at room temperature with different ceramics. The dielectric constant and dielectric loss also have an evident difference with BNT0 doping in NFO. More important, the ME coupling has been found and proved. In our paper, mechanisms explaining the meaningful behaviors are also discussed in detail. Therefore, these results have clear implications for making good use of the BNT0-NFO ceramics with the excellent ferromagnetic, ferroelectric, dielectric properties and the ME coupling effect as long as we can chose the optimal doping content of BNT0.

Acknowledgments This work was supported by the National Natural Science Foundation of China (Grant No. 11174092). We would like to thank the staffs of Analysis Center of HUST for their assistance in various measurements.

References

1. M. Fiebig, *J. Phys. D: Appl. Phys.* **38**, R123 (2005)
2. J. Wang, J.B. Neaton, H. Zheng, V. Nagarajan, S.B. Ogale, B. Liu, D. Viehland, V. Vaithyanathan, D.G. Schlom, U.V. Waghmare, N.A. Spaldin, K.M. Rabe, M. Wuttig, R. Ramesh, *Science* **299**, 1719 (2003)
3. W. Eerenstein, F.D. Morrison, J. Dho, M.G. Blamire, J.F. Scott, N.D. Mathur, *Science* **307**, 1203 (2005)
4. A. Singh, V. Pandey, R.K. Kotnala, D. Pandey, *Phys. Rev. Lett.* **101**, 247602 (2008)
5. N.G. Wang, J. Cheng, A. Pyatakov, A.K. Zvezdin, J.F. Li, L.E. Cross, D. Viehland, *Phys. Rev. B* **72**, 104434 (2005)
6. M. Rawat, K.L. Yadav, *Ceram. Int.* **39**, 3627 (2013)
7. Y. Yuan, C.J. Zhao, X.H. Zhou, B. Tang, S.R. Zhang, *J. Electroceram.* **25**, 212 (2010)
8. A. Ahlawat, V.G. Sathe, V. Ganesan, D.M. Phase, S. Satapathy, *J. Appl. Phys.* **111**, 074302 (2012)
9. J.S. Kim, K.H. Lee, C.I. Cheon, *J. Electroceram.* **22**, 233 (2009)
10. V. Sepelak, D. Baabe, D. Mienert, D. Schultze, F. Krumeich, F.J. Litterst, K.D. Becker, *J. Magn. Magn. Mater.* **257**, 377 (2003)
11. F.L. Zabotto, A.J. Gualdi, J.A. Eiras, A.J.A. Oliveira, D. Garcia, *Mat. Res.* **15**, 428 (2012)
12. Z.M. Tian, S.L. Yuan, X.L. Wang, X.F. Zheng, S.Y. Yin, C.H. Wang, L. Liu, *J. Appl. Phys.* **106**, 103912 (2009)
13. A. Thanaboonsombut, N. Vaneesorn, *J. Electroceram.* **21**, 414 (2008)
14. D.Q. Xiao, D.M. Lin, J.G. Zhu, P. Yu, *J. Electroceram.* **16**, 271 (2006)
15. V.G. Harris, *IEEE Trans. Magn.* **48**, 1075 (2012)
16. T. Kanai, S.I. Ohkoshi, A. Nakajima, T. Watanabe, K. Hashimoto, *Adv. Mater.* **13**, 487 (2001)
17. H.F. Zhang, P.Y. Du, *Solid State Commun.* **149**, 101 (2009)

18. Y.Q. Liu, Y.H. Wu, D. Li, Y.J. Zhang, J. Zhang, J.H. Yang, J. Mater. Sci. Mater. Electron. **24**, 1900 (2013)
19. V. Dorcet, G. Trolliard, P. Boullay, Chem. Mater. **20**, 5061 (2008)
20. D.R. Patil, S.A. Lokare, R.S. Devan, S.S. Chougule, Y.D. Kolekar, B.K. Chougule, J. Phys. Chem. Solid **68**, 1522 (2007)
21. V.R. Palkar, D.C. Kundaliya, S.K. Malik, S. Bhattacharya, Phys. Rev. B **69**, 212102 (2004)
22. C.C. Wang, M.N. Zhang, W. Xia, J. Am. Ceram. Soc. **96**, 1521 (2013)
23. S.K. Choi, B.S. Kang, Y.W. Cho, Y.M. Vysochanskii, J. Electroceram. **13**, 493 (2004)
24. Z. Yu, C. Ang, E. Furman, L.E. Cross, Appl. Phys. Lett. **82**, 790 (2003)
25. D. Viehland, J. Appl. Phys. **88**, 4794 (2000)
26. K.W. Wagner, Ann. Phys. **40**, 818 (1993)